JOURNAL OF THE ROYAL SOCIETY Interface

Site-specific gene transfer with high efficiency onto a carbon nanotube-loaded electrode

Y Inoue, H Fujimoto, T Ogino and H Iwata

J. R. Soc. Interface 2008 **5**, 909-918
doi: 10.1098/rsif.2007.1295

JOURNAL OF THE ROYAL SOCIETY Interface

J. R. Soc. Interface (2008) **5**, 909–918
doi:10.1098/rsif.2007.1295
Published online 11 January 2008

Site-specific gene transfer with high efficiency onto a carbon nanotube-loaded electrode

Y. Inoue[1], H. Fujimoto[1], T. Ogino[2] and H. Iwata[1,*]

[1]*Institute for Frontier Medical Sciences, Kyoto University, 53 Kawahara-cho, Shogoin, Sakyo-ku, Kyoto 606-8507, Japan*
[2]*Department of Electrical and Computer Engineering, Yokohama National University, 79-5 Tokiwadai, Hodogayaku, Yokohama 240-8501, Japan*

A transfection array, which is specifically developed for use in high-throughput analyses of genome functions by the over-expression or suppression of genes on a chip, is expected to become an important method for post-genome research. High efficiency of gene expression or suppression is indispensable for high-throughput analyses because the adherent cell number on a single spot decreases as the density of spots increases in the transfection array. We have studied an electro-stimulated pore formation on the cell membrane for gene delivery. Fine pores should be formed on the cell membrane to increase the efficiency of gene transfection without cell damage. Herein, we examined the electrode carrying chemically functionalized carbon nanotubes (CNTs) on the surface. The CNTs were loaded on a gold electrode with a self-assembled monolayer membrane by electrostatic interaction. Adsorbed plasmid DNA was transfected with higher efficiency into adherent cells on the CNT-loaded electrode than on an electrode without CNTs. This result may be due to the strong but fine field emission formed from the tips of the CNTs.

Keywords: transfection array; electroporation; carbon nanotubes; self-assembled monolayer of alkanethiols

1. INTRODUCTION

Site-specific gene transfer into adherent cells on a substrate, termed transfection array, has been investigated (Palmer & Freeman 2005) since Ziauddin & Sabatini first reported 'reverse transfection' in 2001 (Ziauddin & Sabatini 2001). Transfection array holds great promise as a tool for post-genome research. The functions of genes whose base sequences have been determined in the Human Genome Project (International Human Genome Sequencing Consortium 2001; Tyers & Mann 2003) can be elucidated by their over-expression or suppression. High-throughput transfection array could also be applied to examine protein–protein interaction networks in conjunction with the two-hybrid method (Uetz *et al.* 2000; Suzuki *et al.* 2001). Several methods to immobilize nucleic acids on a substrate for their subsequent transfection into the cells, such as within plasmid and viral DNA or as short interference RNA (siRNA), have been examined to prepare the transfection array. The nucleic acids were immobilized on several kinds of substrates through surface chemical reaction (Ziauddin & Sabatini 2001; Chang *et al.* 2004; Delehanty *et al.* 2004), electrostatic force (Luo & Saltzman 2000; Yamauchi *et al.* 2004*a*; Painnier *et al.* 2005) and biological interactions (Segura *et al.* 2003), and then transfected into the cells through gene transfer methods including usage of a virus carrier (Moffat *et al.* 2006), endocytosis (Segura *et al.* 2003; Chang *et al.* 2004; Delehanty *et al.* 2004; Yamauchi *et al.* 2004*a*; Painnier *et al.* 2005; Fujimoto *et al.* 2006), electropermeation (Yamauchi *et al.* 2004*b*; Ovcharenko *et al.* 2005) and magnetic force (Isalan *et al.* 2005). With the exception of our reported method (Yamauchi *et al.* 2004*b*), non-viral transfection arrays were fabricated based on the endocytosis of cells using cationic liposomes, cationic polymers and their complexes with nucleic acids. Several problems remain to be solved, especially the low expression efficiencies (Hook *et al.* 2006). Our previous studies demonstrated that reverse electroporation should be superior in transfection reproducibility, cell viability, expression efficiency and minimal cross-contamination between spots (Yamauchi *et al.* 2004*b*), and furthermore can control the timing of DNA transfection by applying an electric trigger.

For high-throughput analyses, high expression efficiency is indispensable because the adherent cell number on a single spot decreases as the overall spot density increases on the transfection array. Efficient gene delivery into the cells in a transfection array requires high surface coverage of genes, optimum cell

*Author for correspondence (iwata@frontier.kyoto-u.ac.jp).

Received 8 November 2007
Accepted 15 December 2007

adhesion and spreading, and effective release of the loaded genes. The underlying concept in our reverse electroporation is applying electric potential to the surface to trigger desorption of genes and to transfer them into the adherent cells through the formed pores. In particular, the formation of fine pores on the cell membrane at the application of electric potential is also important to increase the efficiency of gene transfection while decreasing cell damage. Among various parameters for applied electric pulses, electric field strength is the most crucial factor for the formation of pores on the cell membrane. Electric field strength should be in the range from a value that results in a change in cell membrane potential to that leading to permanent irreversible damage to cell membrane structure (Tryfona & Bustard 2005). Carbon nanotubes (CNTs) have the unique properties of their nano-size, high aspect ratio, strong mechanical strength and electric conductivity; therefore CNTs have attracted much attention in the field of not only electronics but also biomedical sciences (Baughman *et al.* 2002; Harrison & Atala 2007). Reverse electroporation using an electrode modified with CNTs could become a promising transfection array owing to their excellent compatibility with cells and biomacromolecules (Dieckmann *et al.* 2003; Hu *et al.* 2004; Gao *et al.* 2006) and the sharp field emission formed from the tip of the CNTs (Choi *et al.* 1999, 2004), which allows fine pores to form on the cell membrane. In this study, we examined a CNT-immobilized surface to improve the expression efficiency. Cells on the CNT electrode, which were transfected with plasmid DNA by the application of electric pulses, expressed proteins efficiently. The results reported here are preliminary, but demonstrate that the CNT-immobilized surface is promising for increasing the expression efficiency.

2. MATERIAL AND METHODS

2.1. Preparation of a CNT-loaded electrode

A CNT-loaded electrode was prepared through the electrostatic interaction between negative charges of the chemically functionalized CNTs and positive charges of the poly(ethyleneimine) (PEI)-adsorbed surface or a self-assembled monolayer (SAM) surface of amino-terminated alkanethiol (NH_2-SAM). The PEI-adsorbed surface was prepared according to the method reported previously (Yamauchi *et al.* 2004*b*). Briefly, a SAM of carboxylic acid-terminated alkanethiol was formed on the gold-evaporated glass plate (thicknesses of chromium and gold were 1 and 49 nm, respectively) in a 1 mM ethanol solution of 11-mercaptoundecanoic acid (Aldrich Chemical Co., St Louis, MO, USA). The gold electrode carrying a SAM of carboxylic acid-terminated alkanethiol (COOH-SAM) was exposed to 10 mg ml^{-1} PEI with an average molecular weight of 25 000 (highly branched PEI) in Dulbecco's phosphate-buffered saline (PBS) solution ([NaCl] = 138 mM; [KCl] = 2.7 mM; [Na_2HPO_4] = 8.1 mM; [KH_2PO_4] = 1.5 mM; pH 7.4) for 30 min, followed by wash of the plate with MilliQ water. The NH_2-SAM was formed on the gold-evaporated glass plate immersed in a 1 mM ethanol solution of 11-amino-1-undecanethiol hydrochloride (Dojindo Laboratories, Kumamoto, Japan).

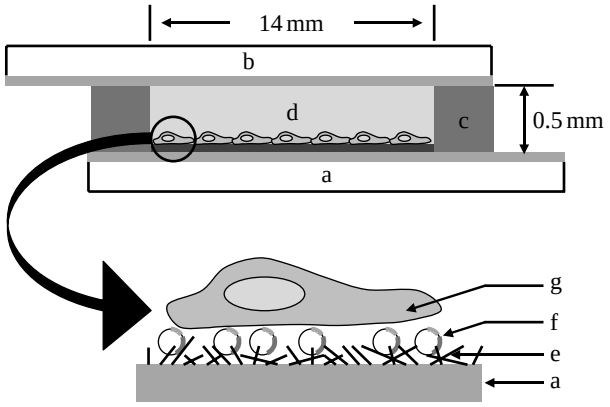

Figure 1. Systematic representation of the apparatus of an electro-stimulated transfection array modified with carbon nanotubes (CNTs). a, CNT-loaded electrode (cathode); b, counter electrode (anode); c, silicone ring; d, PBS (4°C); e, CNTs; f, plasmid DNA; g, cell.

Crude CNTs (multi-walled carbon nanotubes (MWNTs), SES Research, TX, USA, average diameter: 1.2–20 nm, range of length: 100–2000 nm, layer: 5–20 layers) were sonicated in a nitric–sulphuric acid solution (1 : 3 by volume) for 0.5 or 2 hours (Liu *et al.* 1998). After the neutralization of the solution with a NaOH solution, the treated CNTs were isolated by filtration and washed with MilliQ water. The dry functionalized CNTs were obtained by lyophilization. The chemically functionalized CNTs were suspended in MilliQ water. The PEI-adsorbed (PEI/COOH-SAM) or NH_2-SAM electrodes were exposed to the CNT suspension at the concentration of 0.1 mg ml^{-1} for 2 hours. The plates with CNTs were washed with MilliQ water. The obtained CNT-loaded electrodes (CNT/PEI/COOH-SAM or CNT/NH_2-SAM) were stored in ethanol until use.

2.2. Physicochemical characterization of the electrode surface

The loading process of CNTs and subsequent adsorption of plasmid DNA on the electrode were evaluated by a surface plasmon resonance (SPR) apparatus of Kretschmann configuration fabricated in-house (Hirata *et al.* 2000). The PEI in PBS (10 mg ml^{-1}), chemically functionalized CNTs in MilliQ water (0.01, 0.1 and 1.0 mg ml^{-1}) and a plasmid DNA encoding an enhanced green fluorescent protein (EGFP; pEGFP-C1, 4.7 kbp, Clontech Laboratories, Palo Alto, CA, USA) in PBS (5 μg ml^{-1}) were sequentially introduced to the COOH-SAM surface. In the case of the NH_2-SAM surface, the chemically functionalized CNTs in MilliQ water (0.1 mg ml^{-1}) and pEGFP-C1 in PBS (5 μg ml^{-1}) were sequentially introduced. All measurements were performed at 30°C and repeated at least three times.

X-ray photoelectron spectroscopic (XPS) analyses of surfaces were performed using an ESCA-850V (Shimadzu Co., Kyoto, Japan) as follows: a magnesium target was used and the electric current through the

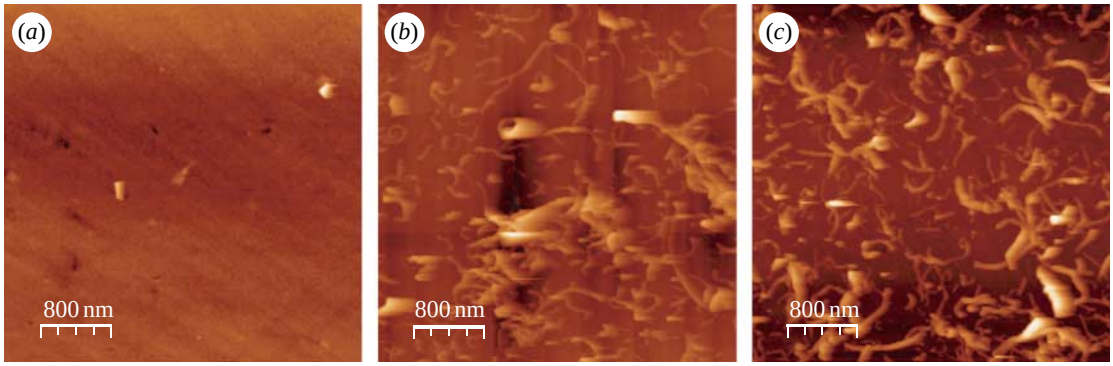

Figure 2. Tapping mode AFM images of different kinds of electrode surfaces. (*a*) COOH-SAM surface, (*b*) CNT/PEI/COOH-SAM surface and (*c*) pEGFP-C1-adsorbed CNT/PEI/COOH-SAM surface. Scale bar, 800 nm.

filament was 30 mA at 8 kV, and the base pressure of the analysis chamber was less than 1×10^{-5} Pa. All spectra shown in the figures were corrected with reference to the peak of Au 4f to 83.8 eV. The XPS measurement was performed for the COOH-SAM, PEI/COOH-SAM, CNT/COOH-SAM and CNT/PEI/COOH-SAM electrodes. The elemental composition of the surfaces was determined from C1s, O1s, N1s, S2p and Au 4f spectra.

Infrared absorption spectra of sample surfaces were collected by the reflection–absorption method using a Spectrum One (Perkin-Elmer, USA) spectrometer equipped with a Reflector (Harrick Sci. Co., NY, USA) and a mercury–cadmium telluride (MCT) detector cooled by liquid nitrogen (FTIR-RAS). Glass plates coated with a layer of gold 199 nm thick were used for FTIR-RAS analyses. Spectra were obtained using the p-polarized infrared laser beam at an incident angle of 75° in the chamber purged with dry nitrogen gas (Taiyo Toyo Sanso Co., Ltd, Osaka, Japan) for 128 scans at 4 cm^{-1} resolution from 4000 to 750 cm^{-1}. The FTIR-RAS measurements were performed for the COOH-SAM, NH_2-SAM, PEI/COOH-SAM, CNT/COOH-SAM, CNT/PEI/COOH-SAM, CNT/NH_2-SAM and pEGFP-C1-adsorbed CNT/PEI/COOH-SAM electrodes, using the bare gold electrode as the reference surface.

2.3. Observation of CNT-loaded electrode surface by atomic force microscopy

An atomic force microscope (AFM; JSPM-5200, JEOL, Tokyo, Japan) was employed to obtain the images of the COOH-SAM, CNT/PEI/COOH-SAM and pEGFP-C1-adsorbed CNT/PEI/COOH-SAM electrodes under the tapping mode in air. Commercially available silicone cantilevers (OMCL-AC160TS, Olympus, Tokyo, Japan) with fundamental resonance frequency of 300 KHz were used. Topographic images were obtained at a scan rate of 2220 nm s^{-1} and a scan area of 4000×4000 nm^2.

2.4. Transfection of plasmid DNA into adherent cells

A plasmid DNA (pEGFP-C1) was transfected into adherent human embryonic kidney (HEK293) cells on the CNT/PEI/COOH-SAM, PEI/COOH-SAM, CNT/NH_2-SAM and NH_2-SAM electrodes by applying an electric pulse (Yamauchi *et al.* 2004*b*). The pEGFP-C1 was adsorbed electrostatically onto the electrode surface in PBS solution at concentrations of 0.5, 5 or 50 μg ml^{-1} (figure 1). The cells were seeded at a density of $2.0–3.0\times10^4$ cells cm^{-2} and cultured using minimal essential medium (MEM) containing 0.1 mg ml^{-1} non-essential amino acids, 10% heat-inactivated foetal bovine serum (FBS), 100 U ml^{-1} penicillin and 0.1 mg ml^{-1} streptomycin. After incubation at 37°C under a 5% CO_2 atmosphere for 24 hours, the MEM was replaced with PBS and a counter electrode (gold-evaporated glass plate; thicknesses of chromium and gold were 1 and 199 nm, respectively) was placed on a silicone frame with the gold surface down. A single pulse was applied using the pulse generator (GenePulser Xcell, Bio-Rad) between an electrode with adherent cells and a counter electrode at the pulse strength of 240 V cm^{-1} for duration of 10 ms at 4°C. After the pulse application, the cells were cultured in MEM for an additional 48 hours. The cells expressing the EGFP were observed using an epifluorescence microscope (BX-71, Olympus) in PBS containing calcium and magnesium ions ($[CaCl_2]=1$ mM, $[MgCl_2]=1$ mM). The cells adherent on the electrodes were collected by trypsinization ([trypsin] = 2.5 mg ml^{-1}, for 3 min at 37°C) and the fraction of cells expressing the EGFP was quantitatively evaluated by the fluorescent-activated cell sorting (FACS) apparatus (FACSCalibur, Becton Dickinson, Franklin Lakes, NJ, USA). Twenty thousand cells were subjected to the FACS counting, with a threshold value between EGFP-positive and -negative cells being determined at the EGFP-negative region containing 99.5% of the non-transfected cells.

2.5. Site-specific gene transfection

Spots containing plasmid DNA were arrayed on a CNT-loaded electrode for the site-specific gene transfer. Glass plates with a gold thin layer were immersed into an ethanol solution of 1-hexadecanthiol (Tokyo Kasei Kogyo Co., Tokyo, Japan) to prepare a SAM carrying methyl groups (CH_3-SAM). The CH_3-SAM surface was irradiated with an ultraviolet light at 180 mW cm^{-2} using an Optical ModuleX (SX-UI 501HQ, Ushio, Inc., Tokyo) equipped with a super-high-pressure mercury lamp (Ushio, Inc.)

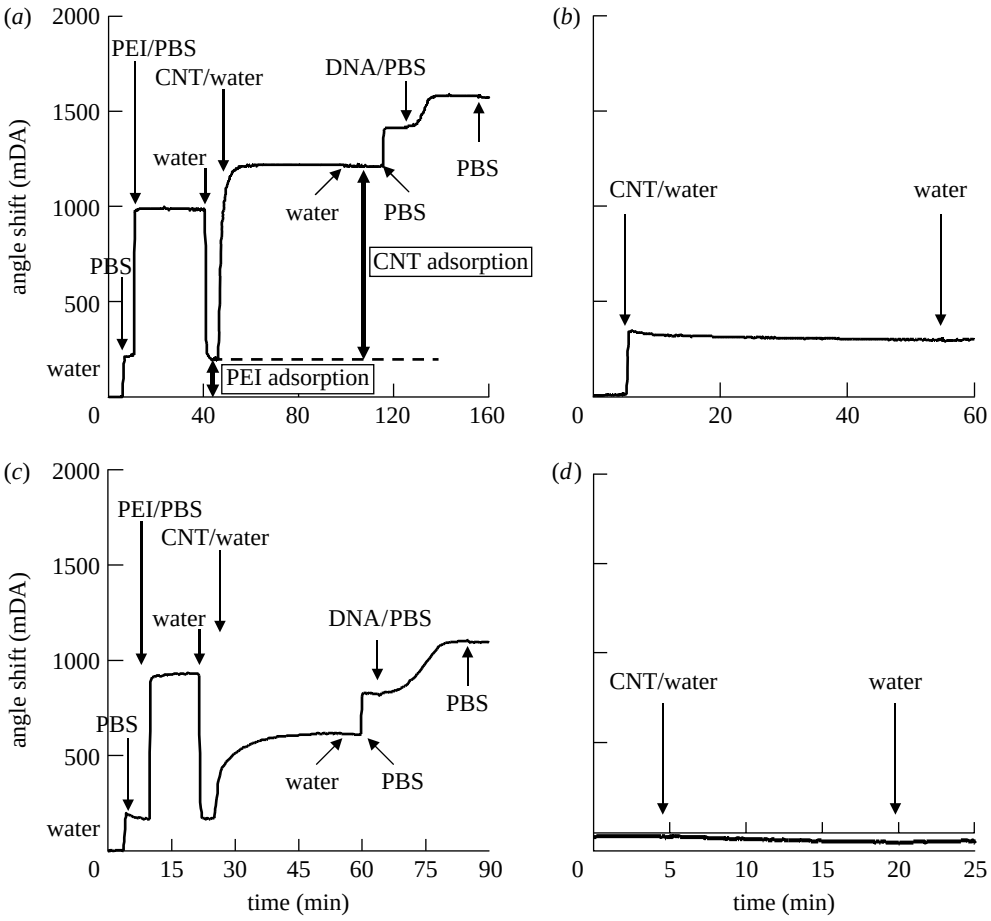

Figure 3. SPR sensorgrams during the exposure of deposition of PEI, chemically functionalized CNTs and plasmid DNA on a COOH-SAM surface. Layer-by-layer membrane formation on a COOH-SAM surface using (*a*) PEI, CNTs chemically functionalized for 0.5 hour, and plasmid DNA, (*b*) direct application of CNTs chemically functionalized for 0.5 hour to the COOH-SAM surface, (*c*) PEI, CNTs chemically functionalized for 2 hours, and plasmid DNA and (*d*) direct application of CNTs chemically functionalized for 2 hours to the COOH-SAM surface.

through a photomask having an array of transparent and circular dots ($\phi = 1$ mm, 5×5 dots) in ambient air for 2 hours. The plates were washed with ethanol to remove photodegradation products and then immersed in an 11-mercaptundecanoic acid solution for 1 hour to form a COOH-SAM within the irradiated regions. The plates were immersed first into a PEI solution and then into a suspension of CNTs as described above. The PBS solutions (5 μg ml^{-1}) of either pEGFP-C1 or pDsRed2-C1 (4.7 kbp, Clontech Laboratories), encoding *Discosoma* sp. red fluorescent protein (DsRed2), were applied to the COOH-SAM spots by manual pipetting. Site-specific gene transfer by an electric pulse was performed as described above except that the pulse duration time was 5 ms. Microscopic observation was performed using an epifluorescence microscope.

3. RESULTS AND DISCUSSION

In this study, chemically functionalized CNTs were loaded onto PEI/COOH-SAM or NH_2-SAM electrodes through the electrostatic interactions between the carboxyl groups on CNTs and the amino groups on the surfaces. Figure 2 shows the AFM images of electrodes with (*a*) COOH-SAM, (*b*) CNT/PEI/COOH-SAM or (*c*) pEGFP-C1-adsorbed CNT/PEI/COOH-SAM.

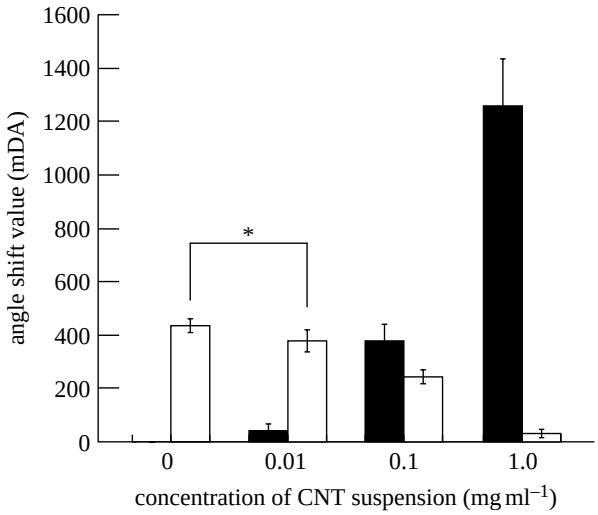

Figure 4. SPR angle shift values caused by the adsorption of CNTs on a PEI-adsorbed electrode surface and plasmid DNA on CNT-loaded electrode surfaces prepared by the application of different kinds of fed concentrations of CNT suspension in MilliQ water (Filled bars, CNTs; open bars, pEGFP-C1; $^{*}p > 0.05$; no significant difference).

Although most of the area of the COOH-SAM surface was smooth (less than 10 nm in height), worm-like structures with various configurations were observed on

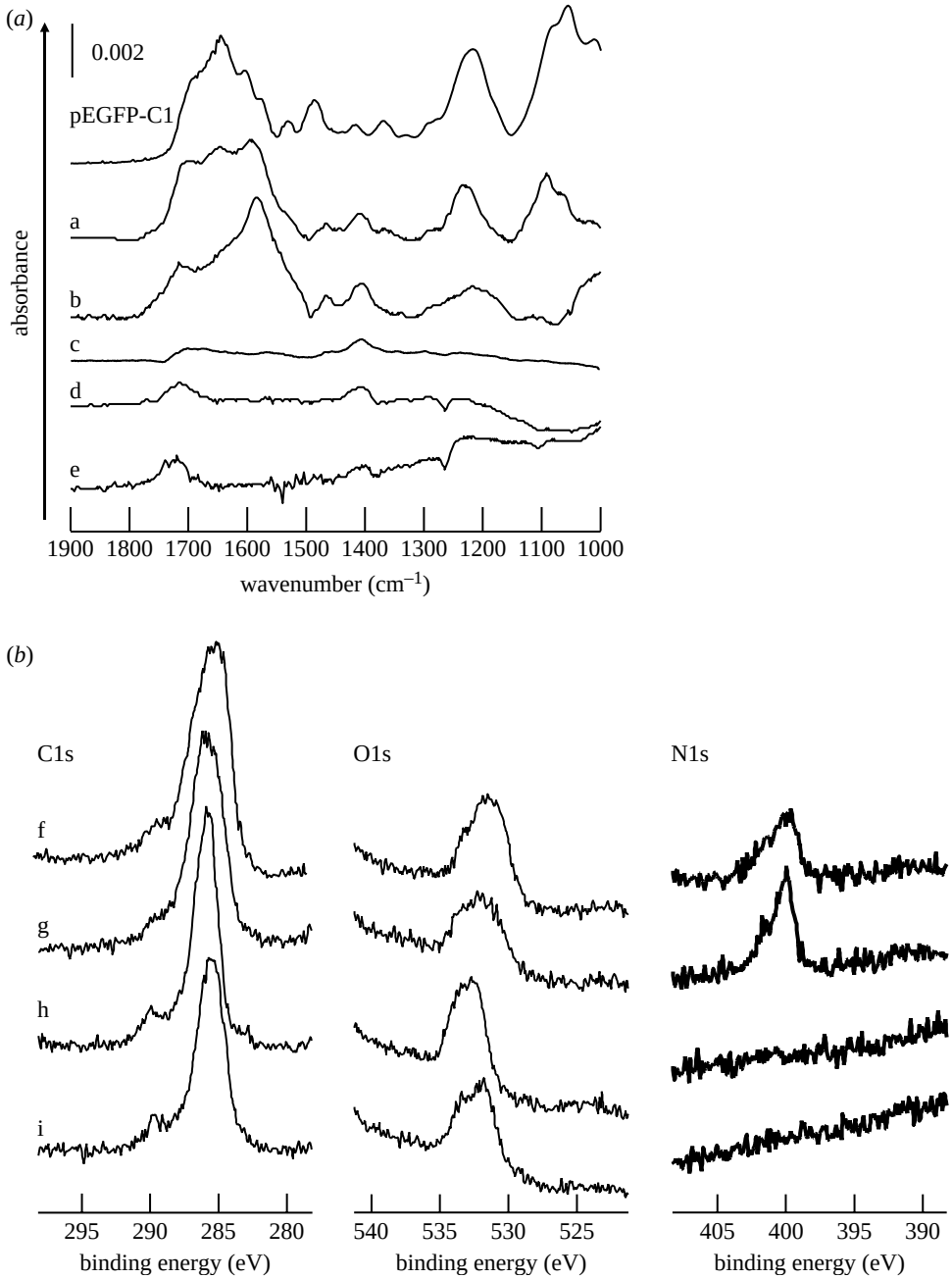

Figure 5. (*a*) FTIR-RAS and (*b*) XPS analyses of electrode surfaces. a, pEGFP-C1-adsorbed CNT/PEI/COOH-SAM electrode; b, f, CNT/PEI/COOH-SAM electrode; c, g, PEI/COOH-SAM surface; d, h, CNT/COOH-SAM electrode; e, i, COOH-SAM electrode. pEGFP-C1, FTIR spectrum of pEGFP-C1 powder. Absorbance was scaled down by one-fifth for easy viewing.

the electrodes with CNTs. Debundled CNTs with a diameter of 25 nm and agglomerated CNTs with the diameter of more than 100 nm were seen in figure 2*b*,*c*.

Figure 3 shows the SPR profiles for CNT adsorption on gold surfaces carrying a COOH-SAM with or without the PEI. Two kinds of the chemically functionalized CNTs with different times for sonication in a strong acid solution (0.5 and 2 hours) were examined in this study. Chemically functionalized CNTs carried carboxyl groups especially at their termini. Strong electrostatic repulsive forces between ionized carboxyl groups suppressed van der Waals attractive forces between CNTs in MilliQ water, while counterions are introduced into the intervening region of CNTs, resulting in shield repulsive forces in PBS. Chemically functionalized

Table 1. Atomic ratios of electrode surfaces calculated from XPS spectra of C1s, O1s and N1s.

electrodes	O/C	N/C	O/N
COOH-SAM	0.16	0.0	—
(theoretical value)	(0.18)	(0)	(—)
CNT/COOH-SAM	0.19	0.0	—
PEI/COOH-SAM	0.14	0.17	0.83
CNT/PEI/COOH-SAM	0.14	0.08	1.76

CNTs could be suspended in MilliQ water, but not in PBS. A PEI solution in PBS was infused onto a COOH-SAM surface. The PEI-adsorbed surface, tube and flow cell were washed with MilliQ water before the flow of CNT suspension in MilliQ water. The SPR profiles

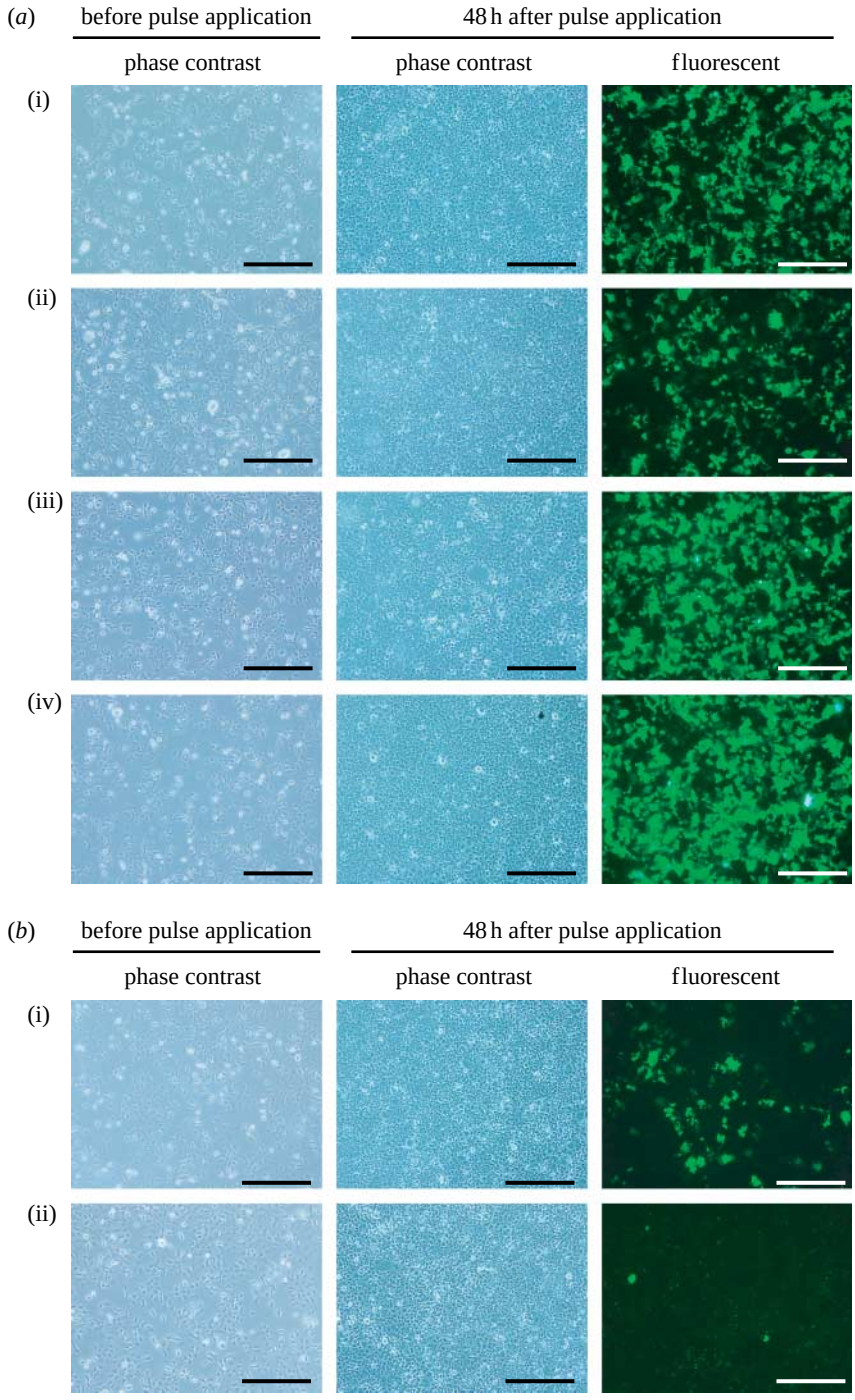

Figure 6. Phase contrast and fluorescent microscopic images of HEK293 cells adhered on pEGFP-C1-adsorbed electrodes. (*a*) CNT/PEI/COOH-SAM and PEI/COOH-SAM electrodes. Plasmid DNA was adsorbed on a CNT/PEI/COOH-SAM electrode at its different concentrations. (i) PEI/COOH-SAM electrode exposed to a solution of 5 μg ml^{-1} plasmid DNA, (ii)–(iv) CNT/PEI/COOH-SAM electrodes were exposed to (ii) a solution of 0.5 μg ml^{-1} plasmid DNA, (iii) a solution of 5 μg ml^{-1} plasmid DNA and (iv) a solution of 50 μg ml^{-1} plasmid DNA. (*b*) CNT/NH_2-SAM and NH_2-SAM electrodes before and at 48 hours after an electric pulse application. (i) NH_2-SAM electrode exposed to a solution of 5 μg ml^{-1} plasmid DNA and (ii) CNT/NH_2-SAM electrode exposed to a solution of 5 μg ml^{-1} plasmid DNA. Scale bar, 500 μm.

containing the flow of the chemically functionalized CNTs treated for 0.5 hour are shown in figure 3*a*,*b*. The angle shift value of the adsorbed PEI onto the COOH-SAM surface was 200 mDA after the wash with MilliQ water (from 0 to 45 min). The temporal increase in the angle shift value at the flow of PEI in PBS solution (1000 mDA) was due to high PEI concentration (10 mg ml^{-1}), known as the bulk effect. The angle shift value, 1000 mDA, was caused by the adsorbed CNTs on the PEI-adsorbed surface (from 45 to 120 min). At the flow of CNT suspension in MilliQ water, a clear bulk effect was not observed due to its low CNT concentration. To see the effect of non-electrostatic interaction, the same CNT suspension in MilliQ water was directly exposed to the COOH-SAM surface, resulting in the angle shift value of 300 mDA (figure 3*b*). The CNT adsorption was caused by van der Waals attractive forces between CNTs and the COOH-SAM surface.

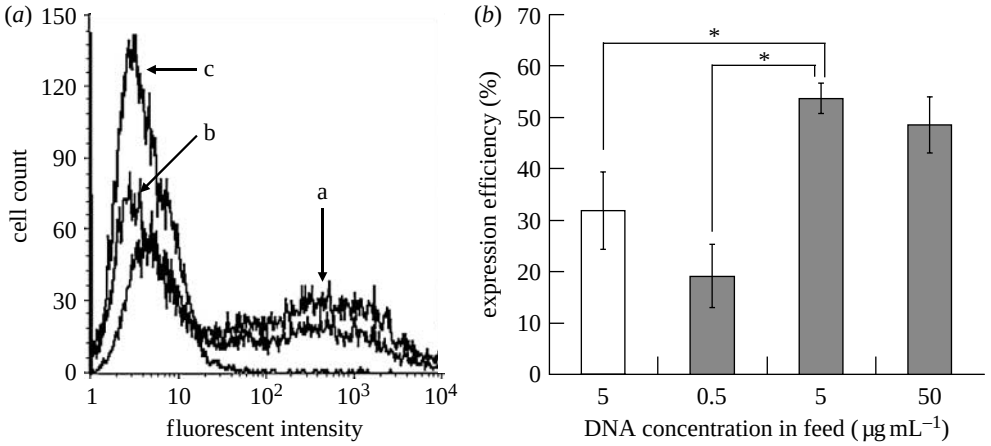

Figure 7. FACS analyses of HEK293 cells transfected with pEGFP-C1 on electrodes. (*a*) Histogram of FACS of live cells transfected on a, CNT/PEI/COOH-SAM; b, PEI/COOH-SAM electrodes; c, native cells. (*b*) Bar chart of GFP expression efficiency. The electrodes were exposed to solutions with different pEGFP-C1 concentrations (open bar, PEI/COOH-SAM; filled bars, CNT/PEI/COOH-SAM; $^{*}p<0.05$).

The effect of the treatment time on CNT adsorption was examined. Figure 3*a*,*b* shows the SPR profiles for the adsorption of CNTs treated for 0.5 hour with strong acid on a COOH-SAM surface with or without PEI treatment. Adsorption of the CNTs was observed on the PEI-treated COOH-SAM surface as shown in figure 3*a*. Although we expect that the electrostatic repulsive force between the chemically functionalized CNTs and the COOH-SAM surface inhibits the adsorption of the CNTs, deposition of the CNTs occurred on the COOH-SAM surface and the angle shift value was 300 mDA as seen in figure 3*b*. The number of carboxyl groups introduced on CNTs treated for 0.5 hour with strong acid was not sufficient to disperse CNT bundles, and thus non-specific deposition of aggregated CNTs occurred on COOH-SAM surfaces with or without PEI treatment. The number of carboxyl groups on the chemically functionalized CNTs is expected to increase with longer treatment in strong acid solution. The SPR profiles for the adsorption of CNTs treated for 2 hours with strong acid are also shown in figure 3*c*,*d*. Adsorption of the CNTs was not observed on the COOH-SAM surface, as shown in figure 3*d*. Increasing carboxyl groups on CNTs induced a strong repulsive force between the CNT itself and the COOH-SAM surface, resulting in the inhibition of CNT adsorption. On the PEI-treated surface, the angle shift value was 400 mDA (from 25 to 60 min), as seen in figure 3*c*. The amount of adsorbed CNTs treated for 2 hours with strong acid was less than half of the CNTs treated for 0.5 hour on the PEI-adsorbed surface. A 2 hour treatment of CNTs with strong acid is sufficient to disperse CNT bundles well and inhibits non-specific deposition of the aggregated CNTs. In the following experiments, CNTs treated for 2 hours with strong acid were used.

When the solution of the plasmid DNA was applied to the CNT-loaded electrode, the SPR angle shift increased with time, indicating that anionic plasmid DNA had adsorbed onto the anionic CNT-loaded electrode. Figure 4 shows the dependence of the adsorbed amounts of CNTs on PEI/COOH-SAM electrodes on the fed concentrations of CNTs in MilliQ water, and also the amounts of plasmid DNA adsorbed on these CNT/PEI/COOH-SAM electrodes. The amount of CNT adsorbed on the electrodes increased with the increase in the fed concentration of CNT in MilliQ water, while the adsorbed amount of the plasmid DNA decreased. As shown in figure 2, the CNTs were clustering on the surface. The plasmid DNA was adsorbed on the PEI surface between the dappled areas covered by the CNTs. The area of PEI-adsorbed surface covered with CNTs enlarged with the increase in the fed concentration of CNT suspension, resulting in a decrease in the plasmid DNA adsorption.

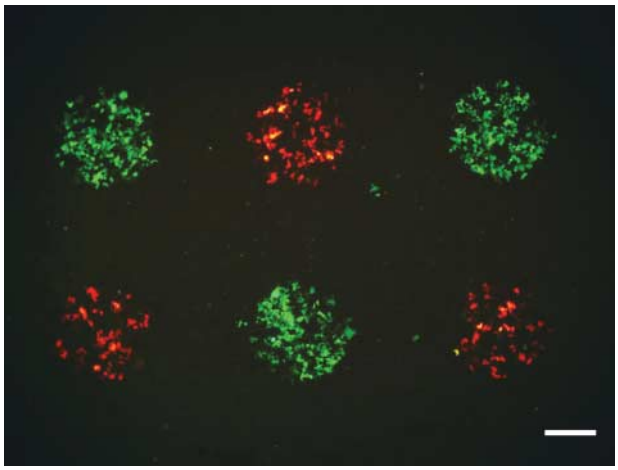

Figure 8. Fluorescent microscopic images of HEK293 cells transfected with pEGFP-C1 or pDsRed2-C1 on a CNT-loaded electrode in an arrayed fashion. Scale bar, 500 μm.

The surface structure of the electrode used in this study was characterized by FTIR-RAS and XPS measurements. In the FTIR-RAS spectra, the CNT/PEI/COOH-SAM electrode surface exhibited a clear absorbance peak at 1585 cm^{-1} (b, figure 5*a*), but the spectra of the PEI/COOH-SAM (c, figure 5*a*) and the CNT/COOH-SAM (d, figure 5*a*) electrodes did not. This peak was developed by the overlap of absorbance bands of the carboxylate ions (Yoo *et al.* 1998) and the carbon skeleton (Shaffer *et al.* 1998). The absorbance peak at 1730 cm^{-1} for the CNT/COOH-SAM electrode was also seen for the COOH-SAM surface (e, figure 5*a*) and is

attributed to the C=O stretching mode of the carboxylic acid. As seen in SPR profiles (figure 3), these results also indicated that a larger quantity of the chemically functionalized CNTs was loaded onto the PEI pre-adsorbed surface than onto the COOH-SAM surface. Clear absorbance peaks were observed at 1095, 1235 and 1649 cm^{-1} for the pEGFP-C1-adsorbed CNT/PEI/COOH-SAM electrode (a, figure 5*a*), but not for the CNT/PEI/COOH-SAM electrode (b, figure 5*a*). These peaks were attributed to symmetric (1095 cm^{-1}) and antisymmetric (1235 cm^{-1}) stretching vibrations of phosphate groups of the DNA backbone, and the vibration mode of amino groups of PEI or nucleotide bases (1649 cm^{-1}), respectively (see also the spectrum of the pEGFP-C1 in figure 5; Zhou & Li 2004). These spectral data confirm that the plasmid DNA was loaded onto the CNT/PEI/COOH-SAM electrode as suggested by the SPR angle shifts (figure 3). Figure 5*b* shows the XPS spectra of C1s, O1s and N1s for surfaces of the given electrodes. Only the electrodes carrying PEI, i.e. the PEI/COOH-SAM and CNT/PEI/COOH-SAM, demonstrated strong N1s signal intensities, but the other two did not. Furthermore, the N1s spectra shapes differed between the PEI/COOH-SAM and the CNT/PEI/COOH-SAM electrodes. A strong peak at 400 eV attributed to the amino group was observed in the N1s spectrum of the PEI/COOH-SAM electrode. For the CNT/PEI/COOH-SAM electrode, the N1s peak shifted to 402 eV, consistent with the presence of a protonated amino group (Ooi *et al.* 2005). Thus, the amino groups in the CNT/PEI/COOH-SAM were more protonated than those in the PEI/COOH-SAM due to the electrostatic interaction between the carboxylic CNTs and the PEI. The atomic ratio of O/C, N/C and O/N ratios obtained from XPS analyses of the four kinds of electrodes were compared (table 1). The O/N value increased from 0.83 to 1.76 by the loading of the CNTs on the PEI/COOH-SAM electrode, reflecting the increased contribution of oxygen from the carboxyl groups in the CNTs.

Figure 6*a* (left column) shows the phase contrast microscopic images of HEK293 cells adhered on the pEGFP-C1-loaded CNT/PEI/COOH-SAM and PEI/COOH-SAM electrodes before the application of an electric pulse. The cells adhered well on these electrodes with high viability (more than 95% determined by propidium iodide (PI) staining), indicating no adverse or toxic effects on the cells by CNTs on the electrodes. In addition, most of the cells (more than 95%, by PI staining) were found to be viable on both the electrodes after the pulse application. The phase contrast (figure 6, centre column) and fluorescent (figure 6, right column) microscopic images of HEK293 cells on the electrode subsequent to the electric pulse showed the successful transfection and expression of pEGFP-C1. Shea *et al.* reported that cells took the plasmid DNA/PEI complex and expressed reporter proteins without the application of an electric pulse (Segura *et al.* 2003), while a limited number of cells expressed EGFP without the application of the electric pulse in this study. The phenomena highly depended on how to deposit the plasmid DNA on the substrate. In their study, the plasmid DNA/PEI complex formed in a solution was applied on the substrate and the cells took plasmid DNA as a complex. On the other hand, PEI and plasmid DNA were applied on the COOH-SAM by the layer-by-layer method, and the plasmid DNA was hardly released from the substrate without an electric pulse in this study. The fluorescent microscopic images showed that the number of cells expressing the EGFP on the CNT/PEI/COOH-SAM electrode increased as a function of the supplied plasmid DNA concentration, reaching a plateau at the concentration of 5 $\mu g\,ml^{-1}$ (figure 6*a*(iii)). Furthermore, under equivalent conditions of the pEGFP-C1 concentration in the feed, the pEGFP-C1 was more efficiently transfected to the cells on the CNT/PEI/COOH-SAM electrode (figure 6*a*(iii)) than those on the electrodes lacking CNTs (figure 6*a*(i)). Thus, the percentage of the EGFP-expressing cells on the CNT/PEI/COOH-SAM electrode was higher than that on the electrode without CNTs. From the quantitative analysis of the fraction of cells expressing EGFP by the FACS measurement (figure 7), the EGFP expression efficiency of the cells on the CNT/PEI/COOH-SAM electrodes increased to 55%, while that on the PEI/COOH-SAM electrodes was 30%. This expression efficiency by reverse electroporation on the CNT-loaded electrode was distinctively higher than that by the reported reverse transfection methods based on cell endocytosis (Hook *et al.* 2006). The HEK293 cells adhered better on the CNT-loaded electrode than on the PEI/COOH-SAM. The CNTs clustering on the surface as seen in figure 2 might stick to the cell membrane (McKnight *et al.* 2003) and thus gene transfer efficiency would increase (Cai *et al.* 2005). The electron transfer between the gold thin film and immobilized CNTs has been reported even in the presence of the insulative SAM layer (Diao & Liu 2005). Therefore, the electric field is expected to localize at the CNT tip and thus it could make fine pores on the cell membrane when an electric pulse was applied. All of these might contribute to increase the expression efficiency of cells on the CNT-loaded electrode.

Figure 6*b* shows phase contrast and fluorescent microscopic images of HEK293 cells adhered on the pEGFP-C1-loaded NH_2-SAM and CNT/NH_2-SAM electrodes before and at 48 hours after the application of an electric pulse. The EGFP expression efficiency of the adherent cells on both electrodes was somewhat lower than that on the PEI-based electrodes as clearly seen in figure 6*a* (NH_2-SAM electrode, less than 5%; CNT/NH_2-SAM electrode, less than 1%). Anionic pEGFP-C1 strongly interacted with highly dense amino groups on the NH_2-SAM surface. The pEGFP-C1 was hardly released from the surface even by the application of an electric pulse. For the case of CNT/NH_2-SAM electrodes, a large amount of the chemically functionalized CNTs were adsorbed on the NH_2-SAM surface, and thus anionic pEGFP-C1 could hardly adsorb on the electrode due to the high coverage of the surface by anionic CNTs.

For site-specific gene transfection, spots with plasmid DNA were arrayed on the CNT-loaded electrodes. Fluorescent microscopic images were acquired 48 hours after the pulse application to cells on the plasmid DNA-arrayed electrode (figure 8). While cell adhesion

occurred over the whole area, as observed by phase contrast microscopy (images were not shown), the EGFP and DsRed2 expressions were observed in an array fashion with high efficiency and with no contamination between the spots.

4. CONCLUSIONS

A CNT-loaded electrode was prepared using the electrostatic interaction between the chemically functionalized CNTs and cationic electrode surface. Cells on the CNT-loaded electrode were transfected with plasmid DNA by applying the electric pulses and they efficiently expressed the proteins by the site-specifically introduced plasmid DNA. These results indicate that reverse electroporation with the CNT-loaded electrodes could be a promising tool for post-genome investigations.

This study was supported in part by the Kobe Knowledge-Based Cluster Creation Project and by a grant-in-aid for Scientific Research (no. 18710098) from the Ministry of Education, Culture, Sports, Science and Technology (MEXT) of Japan. The authors thank Dr Yuji Miyato, Kyoto University, for his assistance during AFM observation.

REFERENCES

Baughman, R. H., Zakhidov, A. A. & de Heer, W. A. 2002 Carbon nanotubes—the route toward applications. *Science* **297**, 787–792. (doi:10.1126/science.1060928)

Cai, D., Mataraza, J. M., Qin, Z.-H., Huang, Z., Huang, J., Chiles, T. C., Carnahan, D., Kempa, K. & Ren, Z. 2005 Highly efficient molecular delivery into mammalian cells using carbon nanotube spearing. *Nat. Methods* **2**, 449–454. (doi:10.1038/nmeth761)

Chang, F.-H., Lee, C.-H., Chen, M.-T., Kuo, C.-C., Chiang, Y.-L., Hang, C.-Y. & Roffler, S. 2004 Surfection: a new platform for transfected cell arrays. *Nucleic Acids Res.* **32**, e33. (doi:10.1093/nar/gnh029)

Choi, W. B. *et al.* 1999 Fully sealed, high-brightness carbon-nanotube field-emission display. *Appl. Phys. Lett.* **75**, 3129–3131. (doi:10.1063/1.125253)

Choi, Y. S. *et al.* 2004 A simple structure and fabrication of carbon-nanotube field emission display. *Appl. Surf. Sci.* **221**, 370–374. (doi:10.1016/S0169-4332(03)00935-8)

Delehanty, J. B., Shaffer, K. M. & Lin, B. 2004 A comparison of microscope slide substrates for use in transfected cell microarrays. *Biosens. Bioelectron.* **20**, 773–779. (doi:10.1016/j.bios.2004.04.016)

Diao, P. & Liu, Z. 2005 Electrochemistry at chemically assembled single-wall carbon nanotube arrays. *J. Phys. Chem. B* **109**, 20 906–20 913. (doi:10.1021/jp052666r)

Dieckmann, G. R. *et al.* 2003 Controlled assembly of carbon nanotubes by designed amphiphilic peptide helices. *J. Am. Chem. Soc.* **125**, 1770–1777. (doi:10.1021/ja029084x)

Fujimoto, H., Yoshizako, S., Kato, K. & Iwata, H. 2006 Fabrication of cell-based arrays using micropatterned alkanethiol monolayers for the parallel silencing of specific genes by small interfering RNA. *Bioconj. Chem.* **17**, 1404–1410. (doi:10.1021/bc060105c)

Gao, L., Nie, L., Wang, T., Qin, Y., Guo, Z., Yang, D. & Yan, X. 2006 Carbon nanotube delivery of the GFP gene into mammalian cells. *Chem. Biol. Chem.* **7**, 239–242.

Harrison, B. S. & Atala, A. 2007 Carbon nanotube applications for tissue engineering. *Biomaterials* **28**, 344–353. (doi:10.1016/j.biomaterials.2007.07.003)

Hirata, I., Morimoto, Y., Murakami, Y., Iwata, H., Kitano, E., Kitamura, H. & Ikada, Y. 2000 Study of complement activation on well-defined surfaces using surface plasmon resonance. *Colloid. Surf. B: Biointerf.* **18**, 285–292. (doi:10.1016/S0927-7765(99)00154-X)

Hook, A. L., Thissen, H. & Voelcker, N. H. 2006 Surface manipulation of biomolecules for cell microarray applications. *Trends Biotechnol.* **24**, 471–477. (doi:10.1016/j.tibtech.2006.08.001)

Hu, H., Ni, Y., Montana, V., Haddon, R. C. & Parpura, V. 2004 Chemically functionalized carbon nanotubes as substrates for neuronal growth. *Nano Lett.* **4**, 507–511. (doi:10.1021/nl035193d)

International Human Genome Sequencing Consortium 2001 Initial sequencing and analysis of the human genome. *Nature* **409**, 860–921. (doi:10.1038/35057062)

Isalan, M., Santori, M. I., Gonzalez, C. & Serrano, L. 2005 Localized transfection on arrays of magnetic beads coated with PCR products. *Nat. Methods* **2**, 113–118. (doi:10.1038/nmeth732)

Liu, J. *et al.* 1998 Fullerene pipes. *Science* **280**, 1253–1256. (doi:10.1126/science.280.5367.1253)

Luo, D. & Saltzman, W. M. 2000 Enhancement of transfection by physical concentration of DNA at the cell surface. *Nat. Biotechnol.* **18**, 893–895. (doi:10.1038/78523)

McKnight, T. E. *et al.* 2003 Intracellular integration of synthetic nanostructures with viable cells for controlled biochemical manipulation. *Nanotechnology* **14**, 551–556. (doi:10.1088/0957-4484/14/5/313)

Moffat, J. *et al.* 2006 A lentiviral RNAi library for human and mouse genes applied to an arrayed viral high-content screen. *Cell* **124**, 1283–1298. (doi:10.1016/j.cell.2006.01.040)

Ooi, Y., Hobara, D., Yamamoto, M. & Kakiuchi, T. 2005 Ideal nonideality in adsorption of 2-aminoethanethiol and 2-mercaptoethane sulfonic acid to form electrostatically stabilized binary self-assembled monolayers on Au(111). *Langmuir* **21**, 11 185–11 189. (doi:10.1021/la051160x)

Ovcharenko, D., Jarvis, R., Hunicke-Smith, S., Kelnar, K. & Brown, D. 2005 High-throughput RNAi screening *in vitro*: from cell lines to primary cells. *RNA* **11**, 985–993. (doi:10.1261/rna.7288405)

Painnier, A. K., Anderson, B. C. & Shea, L. D. 2005 Substrate-mediated delivery from self-assembled monolayers: effect of surface ionization, hydrophilicity, and patterning. *Acta Biomater.* **1**, 511–522. (doi:10.1016/j.actbio.2005.05.004)

Palmer, E. & Freeman, T. 2005 Cell-based microarrays: current progress, future prospects. *Pharmacogenomics* **6**, 527–534. (doi:10.2217/14622416.6.5.527)

Segura, T., Volk, M. J. & Shea, L. D. 2003 Substrate-mediated DNA delivery: role of the cationic polymer structure and extent of modification. *J. Control. Release* **93**, 69–84. (doi:10.1016/j.jconrel.2003.08.003)

Shaffer, M. S. P., Fan, X. & Windle, A. H. 1998 Dispersion and packing of carbon nanotubes. *Carbon* **36**, 1603–1612. (doi:10.1016/S0008-6223(98)00130-4)

Suzuki, H. *et al.* 2001 Protein–protein interaction panel using mouse full-length cDNAs. *Genome Res.* **11**, 1758–1765. (doi:10.1101/gr.180101)

Tryfona, T. & Bustard, M. T. 2005 Enhancement of biomolecule transport by electroporation: a review of theory and practical application to transformation of *Corynebacterium glutamicum*. *Biotechnol. Bioeng.* **93**, 413–423. (doi:10.1002/bit.20725)

Tyers, M. & Mann, M. 2003 From genomics to proteomics. *Nature* **422**, 193–197. (doi:10.1038/nature01510)

Uetz, P. *et al.* 2000 A comprehensive analysis of protein–protein interactions in *Saccharomyces cerevisiae*. *Nature* **403**, 623–631. (doi:10.1038/35001009)

Yamauchi, F., Kato, K. & Iwata, H. 2004*a* Micropatterned, self-assembled monolayers for fabrication of transfected cell microarrays. *Biochim. Biophys. Acta* **1672**, 138–147.

Yamauchi, F., Kato, K. & Iwata, H. 2004*b* Spatially and temporally controlled gene transfer by electroporation into adherent cells on plasmid DNA-loaded electrodes. *Nucleic Acids Res.* **32**, e187. (doi:10.1093/nar/gnh176)

Yoo, D., Shiratori, S. S. & Rubner, M. F. 1998 Controlling bilayer composition and surface wettability of sequentially adsorbed multilayers of weak polyelectrolytes. *Macromolecules* **31**, 4309–4318. (doi:10.1021/ma9800360)

Zhou, Y. & Li, Y. 2004 Studies of interaction between poly(allylamine hydrochloride) and double helix DNA by spectral methods. *Biophys. Chem.* **107**, 273–281. (doi:10.1016/j.bpc.2003.09.009)

Ziauddin, J. & Sabatini, D. M. 2001 Microarrays of cells expressing defined cDNAs. *Nature* **411**, 107–110. (doi:10.1038/35075114)